
Prediction of subsurface damage depth of ground brittle materials by surface profiling

Tsutomu Ohta

Mitsubishi Electric Corporation,
Kamakura Works,
325 Kamimachiya,
Kamakura, Kanagawa 247-8520, Japan

Jiwang Yan* and Tsunemoto Kuriyagawa

Department of Nanomechanics,
Tohoku University,
Aramaki Aoba 6-6-01, Aoba-ku,
Sendai 980-8579, Japan
E-mail: yanjw@pm.mech.tohoku.ac.jp
*Corresponding author

Sunao Kodera

Mitsubishi Electric Corporation,
Kamakura Works,
325 Kamimachiya,
Kamakura, Kanagawa 247-8520, Japan

Tomoaki Nakasuji

Mitsubishi Electric Corporation,
Manufacturing Engineering Centre,
8-1-1, Tsukaguch-Honmachi, Amagasaki,
Hyogo 661-8661, Japan

Abstract: In the manufacturing of infrared optics, grinding is usually used as a premachining process for generating aspherical lens figures on brittle materials such as germanium and silicon before diamond turning or polishing. However, microcracks will be generated in workpiece materials by the grinding process. The subsurface crack depth determines the depth of material removal of the finishing processes and affects the total manufacturing time. In order to minimise the depth of finishing removal, it is important to know the grinding-induced crack depth accurately. In this paper, we attempt to predict the subsurface damage depth by surface profiling techniques. The surface roughness of ground silicon and germanium was measured by a stylus-type profilometer with different stylus geometries and the subsurface crack depth was evaluated using two different methods, namely, small-tool polishing method and slanted-polishing method. The relationship between the surface roughness and the subsurface crack depth was experimentally investigated.

Keywords: silicon; germanium; infrared lens; diamond turning; grinding; surface roughness; subsurface damage; microcrack.

Reference to this paper should be made as follows: Ohta, T., Yan, J., Kuriyagawa, T., Kodera, S. and Nakasuji, T. (2007) 'Prediction of subsurface damage depth of ground brittle materials by surface profiling', *Int. J. Machining and Machinability of Materials*, Vol. 2, No. 1, pp.108–124.

Biographical notes: Tsutomu Ohta graduated from Ritsumeikan University with a Master's degree in 1988 and a Bachelor's degree in 1986, both in Mechanical Engineering. He joined Mitsubishi Electric Corporation Kamakura Works in 1988. He has been a Manager of Manufacturing Engineering section since 2001 and a student of doctor courses in Tohoku University since 2006. He has been engaged in development of high efficiency and accuracy and precision machining.

Jiawang Yan is an Associate Professor in the Department of Nanomechanics, Graduate School of Engineering, Tohoku University, Japan. His research interests include ultraprecision machining of optical and optoelectronic materials, design and fabrication of nano-structural surfaces, micro/nano-machining mechanics and machining damages of crystals and semiconductors.

Tsunemoto Kuriyagawa is a Professor in the Department of Nanomechanics, Graduate School of Engineering, Tohoku University, Japan. His research interests include nano-precision mechanical fabrication and micro/meso mechanical manufacturing (M4 process).

Sunao Kodera is a Head Engineer of the Kamakura Works, Mitsubishi Electric Corporation. He graduated from Kanazawa University with a Master's degree in 1983 and a Bachelor's degree in 1981, both in Precision Engineering. He has been engaged in development of material processing of optical components.

Tomoaki Nakasuji received a BE (1984) and an ME (1986) in Mechanical Engineering from Osaka University, Osaka, Japan. He joined the Manufacturing Development Laboratory (now Manufacturing Engineering Centre), Mitsubishi Electric Corporation Hyogo, Japan, in 1986. He has been engaged in development of high efficiency and accuracy and precision machining.

1 Introduction

Recently, various high-precision infrared optical lenses are required in thermal imaging systems, dark-field sensing systems and night vision systems of vehicles. These lenses are required to have both high form accuracy and high surface quality. Diamond turning and polishing are two major fabrication methods usually used to manufacture such infrared lenses on brittle materials such as single-crystalline germanium and silicon (Suzuki et al., 1997; Yan et al., 2001, 2002, 2005). To reduce production cost, grinding is usually used as a premachining process to generate the rough lens figures at a high material removal rate in the beginning of the lens manufacturing process. On most occasions, damages will be generated to the workpiece materials during the grinding process and these damages must be removed by the subsequent finishing processes.

Generally speaking, machining-induced damages involve two aspects: one is 'surface damages' which can be observed from the surface and the other is called 'subsurface damages', which are invisible from the surface. The subsurface damages may include dislocations, phase transformations and microcracks extending downwards into the work material (Pei et al., 1999; Yan, 2004; Yan et al., 2005; Zhang et al., 2003). For most mechanical or optical applications, the damages due to microcracks are fatal problems for the function of a component. When microcracks occur during machining, the machining regime is called 'brittle mode machining'; while if no crack appears, the machining mode will be considered to be 'ductile regime machining'. Compared to microcracks, dislocations and phase transformations are relatively slight damages, which occur even in the 'ductile regime machining' (Yan, 2004). The influence of dislocations and phase transformations is an item to concern after the microcracks have been completely removed. In this paper, we emphatically investigated the subsurface microcracks caused by grinding.

To remove the grinding-induced microcracks from the lens substrates, diamond turning technique is usually used, where extremely sharp single-crystalline diamond tools and ultraprecision lathes with high stiffness are required (Yan et al., 2001, 2002, 2005). However, the wear of diamond tools during ductile machining is serious compared to that in metal machining. Therefore, in general, the total cutting distance of a diamond tool must be shorter than a critical value to achieve high quality optical surfaces (Yan et al., 2003). In order to shorten the cutting distance for machining an optical lens with certain diameter, an effective way is to use a high tool feed rate (Yan et al., 2002). Another approach should be to minimise the number of tool passes needed for removing the grinding-induced microcracks. For the later, it is important to know the maximum depth of subsurface cracks to determine the tool pass numbers. However, to date, there has not been practical, rapid and non-destructive method for measuring the grinding-induced crack depth accurately in the micrometer level.

In this paper, we attempt to predict the depth of the grinding-induced microcracks using the surface roughness information. For this purpose, the relationship between the surface roughness and the subsurface crack depth of ground silicon and germanium lens substrates was experimentally investigated. The surface roughness was measured by a stylus-type profilometer with different stylus geometries. The subsurface crack depth was evaluated using two different methods, namely, small-tool polishing method and slanted-polishing method. The effect of abrasive grain size on the crack depth was also investigated.

2 Grinding experiments

The work materials were optical grade silicon (Ge) and silicon (Si), having surface crystal orientations of (111). The workpieces were 25 mm in diameter and 3 mm in thickness. Flat surfaces were formed by a precision grinding machine, as given in Figure 1. Figure 2 shows the geometry of the cup-type grinding wheel. Four kinds of wheels, given in Table 1, were used. The grinding conditions are given in Table 2. These grinding conditions provide a situation that the average material removal volume per abrasive grain was almost the same for different wheels during finish grinding (Matsui, 1999).

Figure 1 Schematic diagram of the grinding set-up

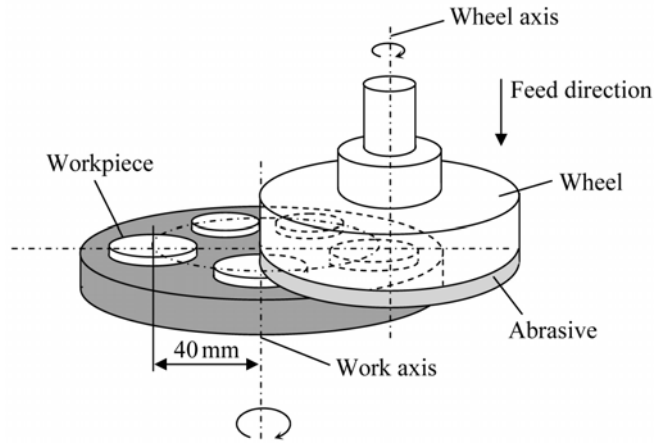


Figure 2 Grinding wheel shape

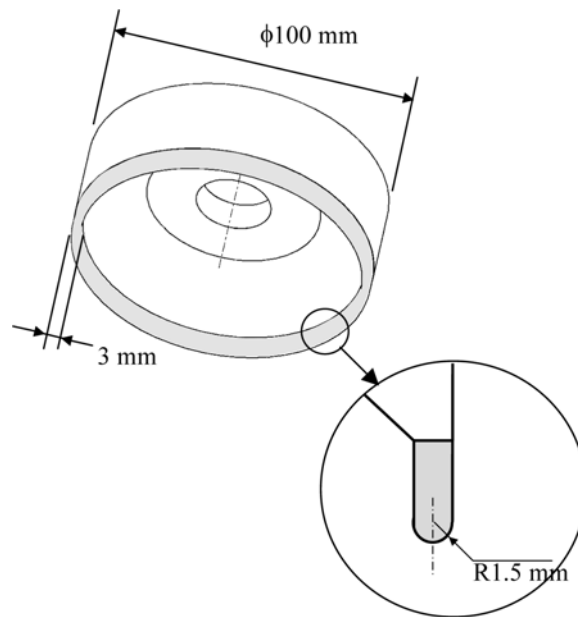


Table 1 Grinding wheel specifications

| Type | Purpose of use | Abrasive grain material | Average abrasive diameter (μm) | Bond type |
|------|----------------|-------------------------|---|-----------|
| 1 | Rough | Synthetic diamond | 149 | Metal |
| 2 | Semifinish | | 20 | Metal |
| 3 | Finish | | 10 | Resin |
| 4 | Finish | | 8 | Resin |

Table 2 Grinding conditions

| | 149 μm | | 20 μm | | 10 μm | | 8 μm | |
|---------------------------|-------------------|--------------------|-------------------|--------------------|-------------------|--------------------|-------------------|--------------------|
| | Depth of cut (mm) | Feed rate (mm/min) | Depth of cut (mm) | Feed rate (mm/min) | Depth of cut (mm) | Feed rate (mm/min) | Depth of cut (mm) | Feed rate (mm/min) |
| Rough | | | | 0.04 | | 0.005 | | 0.005 |
| Semifinish | 0.2 | 0.2 | 0.05 | 0.02 | 0.005 | 0.005 | 0.005 | 0.005 |
| Finish | | | | 0.02 | | 0.005 | | 0.003 |
| Spark out time (sec) | 90 | | 90 | | 120 | | 120 | |
| Wheel spindle speed (rpm) | 4600 | | 4600 | | 4600 | | 4600 | |
| Work spindle speed (rpm) | 6.5 | | 4 | | 4 | | 4 | |

Three kinds of evaluation methods were selected to evaluate the ground surfaces: stylus profiling method for surface roughness measurement, small-tool polishing removal method and slanted-polishing method for evaluating the depth of the microcracks. The details and the results of the three methods are given as follows.

3 Surface roughness measurement

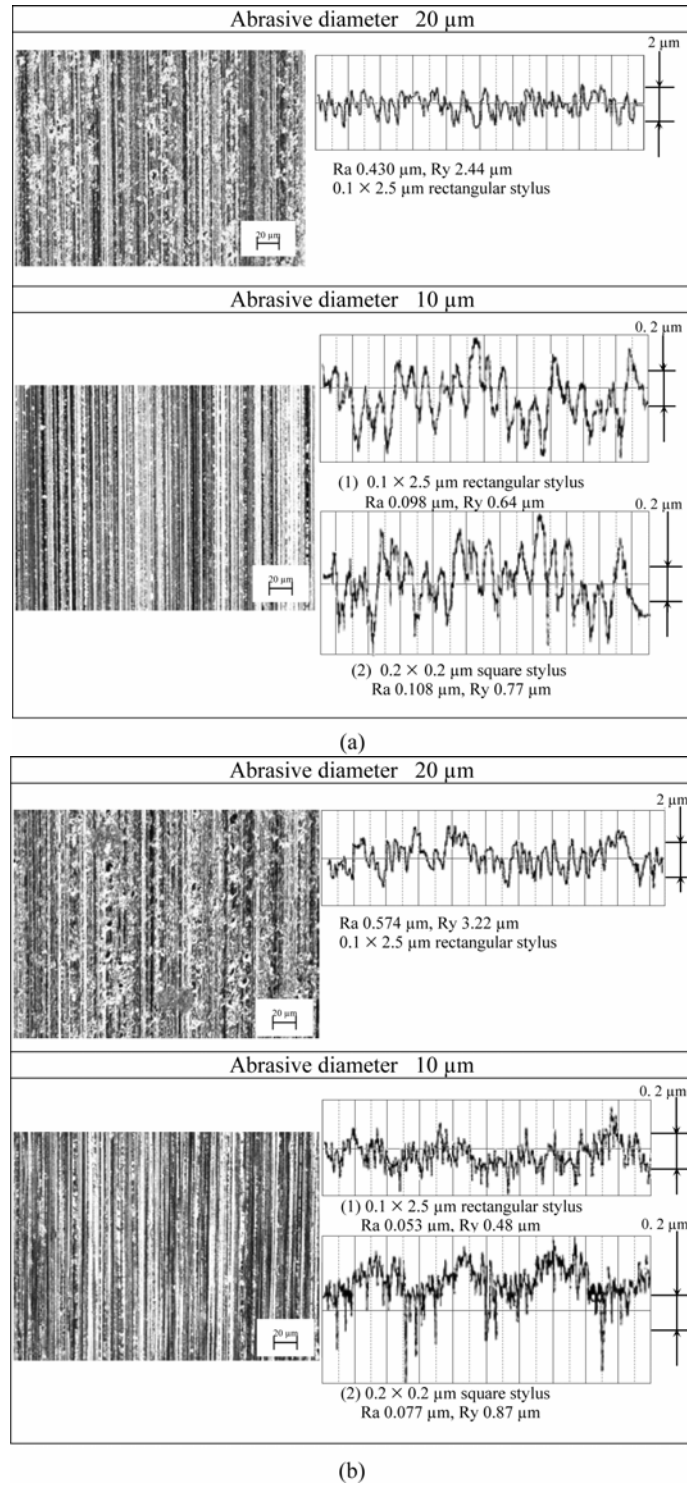
3.1 Measurement procedures

A contact-type stylus profilometer, Talystep, made by Taylor Hobson Co. Ltd., was used to measure surface roughness. First, a $0.1 \times 2.5 \mu\text{m}$ rectangular type of stylus was used. Its long side ($2.5 \mu\text{m}$) traversed perpendicularly to the grinding mark. A $0.2 \times 0.2 \mu\text{m}$ square stylus was then used for comparison. One side of the stylus traversed perpendicularly and the other side traversed parallel to the grinding mark. Both traverse lengths were 1 mm. Different types of styli were used to compare the measurement results. The small square stylus was only used to evaluate the roughness of surfaces ground by the grinding wheels with 8 and 10 μm abrasive diameters, because the stylus might be damaged when measuring the rougher surfaces ground by larger abrasives.

3.2 Measurement results

Figure 3(a) and (b) shows micrographs and measurement results of germanium and silicon surfaces ground by the 20- and 10- μm diameter abrasive wheels, respectively. Both germanium and silicon surfaces ground by the 20- μm diameter abrasive show brittle regime appearances. The surface roughness was 2.44–3.22 μm Ry. On the other hand, the brittle fractures decreased on the surfaces ground by the 10- μm abrasives. Smooth grinding traces become clearly seen, compared with surfaces machined by the 20- μm diameter abrasives. The surface roughness was 0.67–0.87 μm Ry.

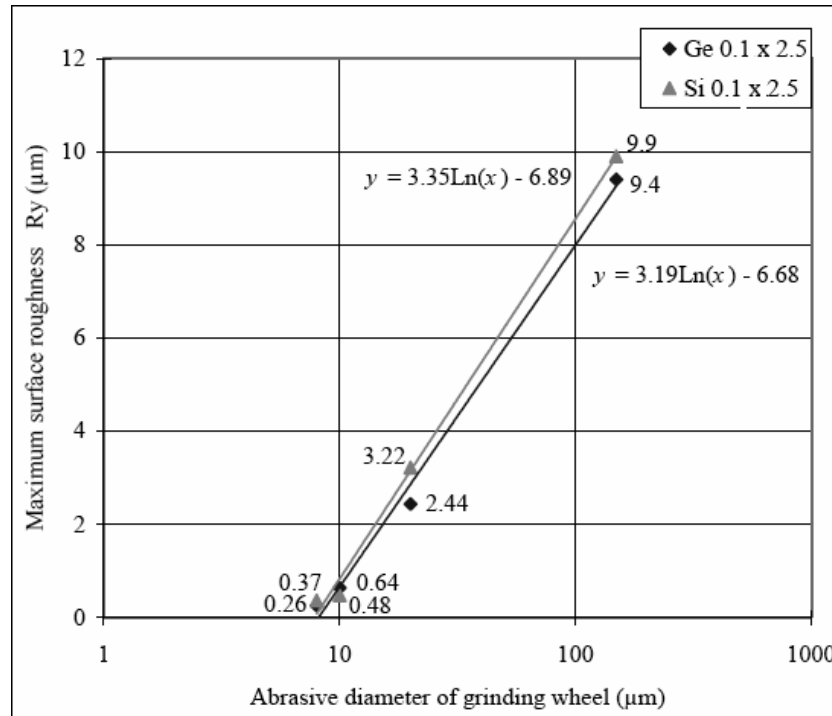
Figure 3 Micrographs and cross-sectional profiles of ground surfaces of germanium (a) and silicon (b)



3.3 Analysis of measurement results

Figure 4 shows the surface roughness of germanium and silicon plotted in the one-axis logarithmic graph. The horizontal axis is the abrasive diameter of the grinding wheel. The vertical axis is the maximum surface roughness R_y .

Figure 4 Surface roughness measured by Talystep with the $0.1 \times 2.5 \mu\text{m}$ rectangular stylus



It can be seen that the maximum surface roughness R_y increases with the increase of the abrasive diameter and the two parameters have a logarithmically linear relationship. For silicon, the relationship between the surface roughness and the abrasive diameter can be described by the following logarithmic function.

$$y = 3.35\text{Ln}(x) - 6.89 \quad (1)$$

For germanium, the relationship between the surface roughness and the abrasive diameter can be described by the following equation.

$$y = 3.19\text{Ln}(x) - 6.68 \quad (2)$$

Figure 5 is a comparison of the results measured by two different styli, $0.2 \times 0.2 \mu\text{m}$ and $0.1 \times 2.5 \mu\text{m}$. Generally speaking, the $0.2 \times 0.2 \mu\text{m}$ stylus results were larger than the $0.1 \times 2.5 \mu\text{m}$ results. The $0.2 \times 0.2 \mu\text{m}$ result of the 10- μm abrasive diameter for silicon was 1.8 times larger than the $0.1 \times 2.5 \mu\text{m}$ result and the others were 1.2 times larger. These results show that surface roughness measured by scanning the stylus to the work surface change significantly with the stylus shape and size (Thomas, 1999).

Figure 5 Comparison of results measured by different styli ($0.1 \times 2.5 \mu\text{m}$ and $0.2 \times 0.2 \mu\text{m}$, traverse length 1 mm)

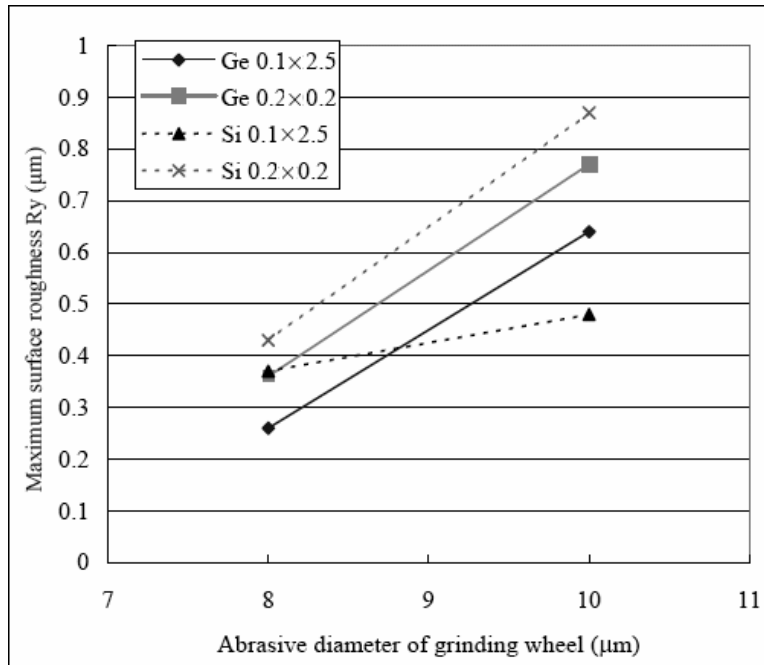


Figure 6 is a schematic illustration that shows the measurement result change with the difference in the stylus geometry. The sharper stylus can enter into the microcraters much deeper, thus can measure the depth of craters, that is, the real surface roughness, more accurately. Especially for the brittle-regime machined surface, where very narrow and deep cracks occur into the surface, the difference in surface roughness measured by different styli becomes very significant. As shown in Figure 3, for the same surface ground by the $10\text{-}\mu\text{m}$ abrasive, the surface roughness profile of $0.2 \times 0.2 \mu\text{m}$ stylus indicates some deep scratches and cracks; whereas the result of $0.1 \times 2.5 \mu\text{m}$ stylus shows a relatively smooth surface and does not indicate any deep surface features.

4 Subsurface crack depth evaluation

4.1 Small-tool polishing method

Next, we measured the subsurface crack depth using the small-tool polishing method. At first, a small rotating tool was made of urethane to polish the ground workpiece surface to form a small depression and then the crack depth was evaluated by observing the cracks shown on the depression surface.

The small polishing tool was 6 mm in diameter and fabricated by diamond turning. The tool was rotated at 1000 rpm. A 100-g polishing force was acted to the tool to remove a thin layer of material from the workpiece and generate a shallow depression via abrasives, as shown in Figure 7. The polished volume was adjusted by the polishing time.

Figure 6 Schematic of surface profiling mechanism with different styli

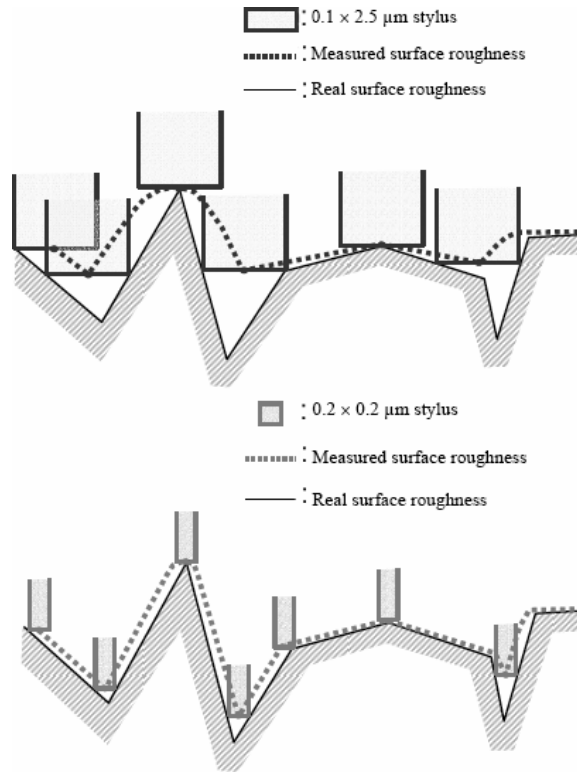


Figure 7 Schematic illustration of the polishing head

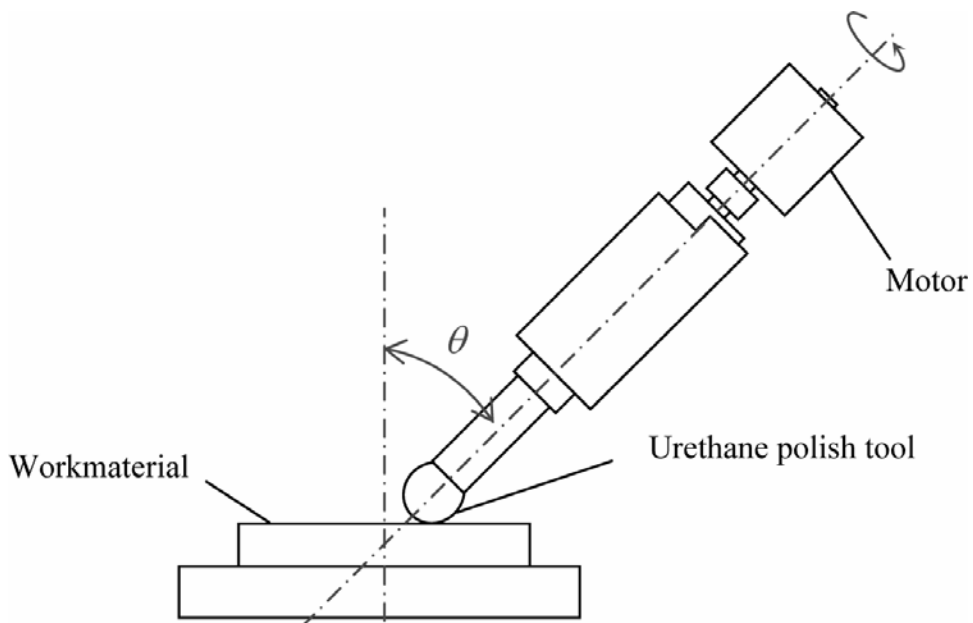


Figure 8 shows a schematic illustration of the polished surface. The boundary area A between the ground area and crack-free area was observed and measured by an optical microscope. Then l was measured by another surface profilometer, Form Talysurf, which can be used to measure curved surfaces. Colloidal SiO_2 was used as abrasives in the polishing slurry. This slurry is usually used to eliminate the cutter marks formed on silicon workpieces caused by diamond turning (Yan et al., 2002). The diameter of the abrasive was $0.08 \mu\text{m}$.

Figure 8 Schematic of a depression polished by the small tool

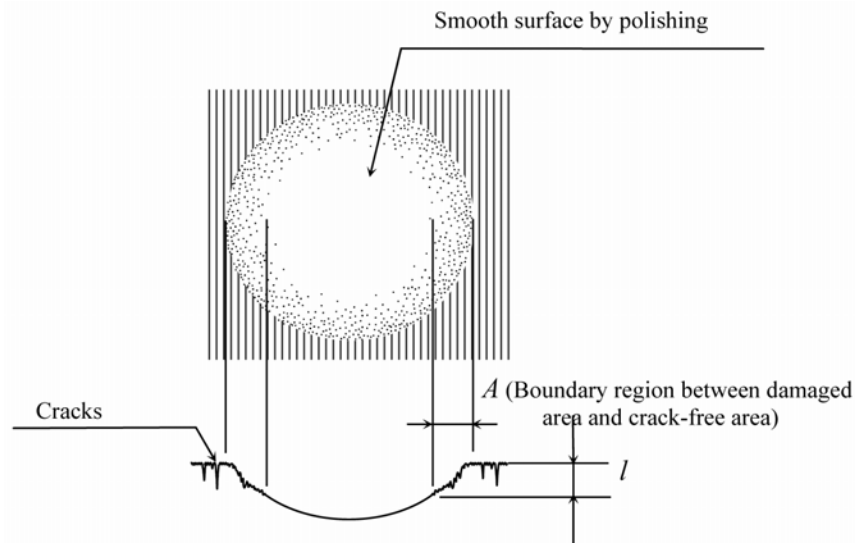


Figure 9 shows a micrograph of the polished depression on a silicon surface ground by $20\text{-}\mu\text{m}$ diameter abrasives. The surface polished by the small polish tool has a crack-free area in the centre. The smooth mirror surface region is shown as the black part in the figure. The cracks are shown as the white spots in the boundary area between the ground and crack-free area. Figure 10 is an enlarged micrograph of the boundary area. In this figure, the smooth mirror surface region is shown as the white part and cracks are shown as the black spots in the boundary area. The inverse contrast against Figure 9 was caused by the difference of the sample tilting angle and the light reflection effects. The crack depth was determined by examining the place at which cracks occurred. Then, the depth was measured from the profile of Form Talysurf. In order to examine the reliability of this evaluation method, the crack depth of the same surface was measured at various polishing time to see if there is any change in the results. The results showed that the repetitive measurement accuracy of crack depth by this method was about $1 \mu\text{m}$.

4.2 Slanted-polishing method

To compare with the small-tool polishing method, slanted-polishing method was also used to evaluate the subsurface crack depth. As shown in Figure 11, the ground surface was at first polished with a flat polishing pad at a slant. Then a microscope and Form Talysurf were then used to observe and measure the distances a and l .

The crack depth was then calculated from the value of a and l . The slant angle θ was about 1° in the present experiment, so that the removal volume was more than $100\ \mu\text{m}$ at the end of sample. The material removal volume in this method is far larger than that in the small-tool method, thus a high material removal rate is preferable. For this reason, diamond paste was selected as abrasives. The polish conditions are given in Table 3.

Figure 9 Micrograph of the depression surface polished by the small tool

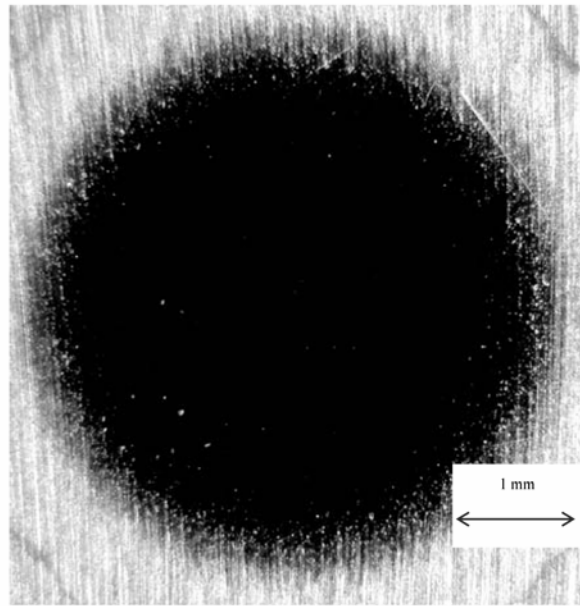


Figure 10 Boundary area between the ground area and crack-free area

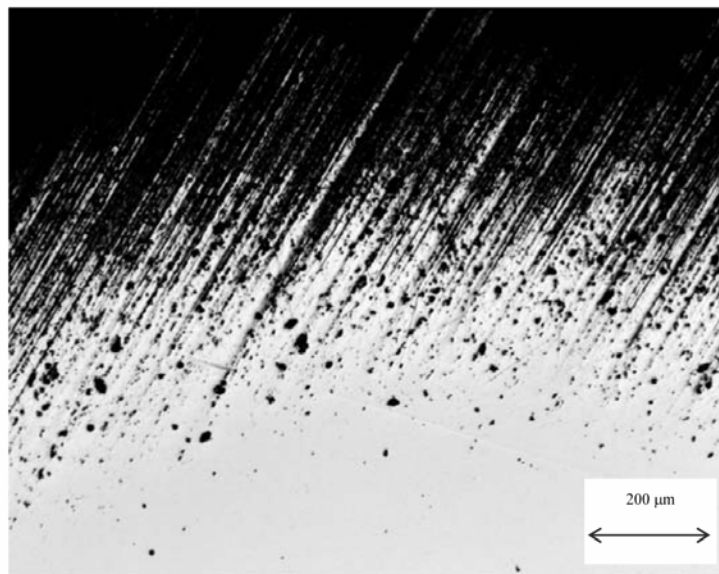


Figure 11 Schematic illustration of a sample made by slanted polishing

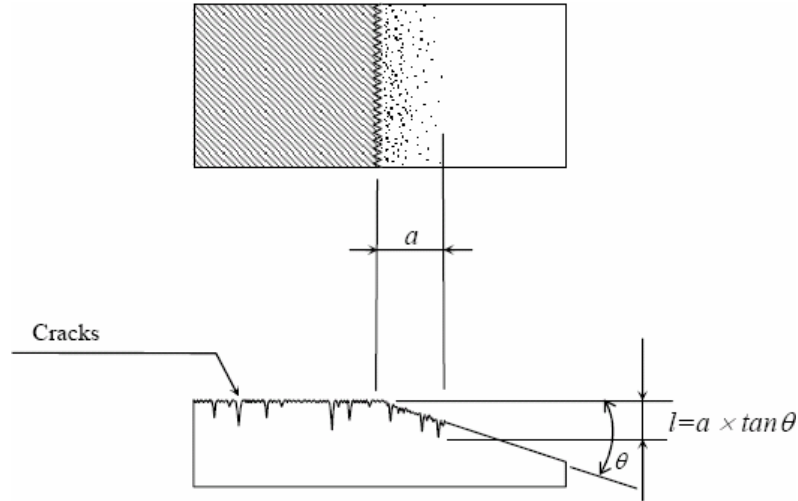
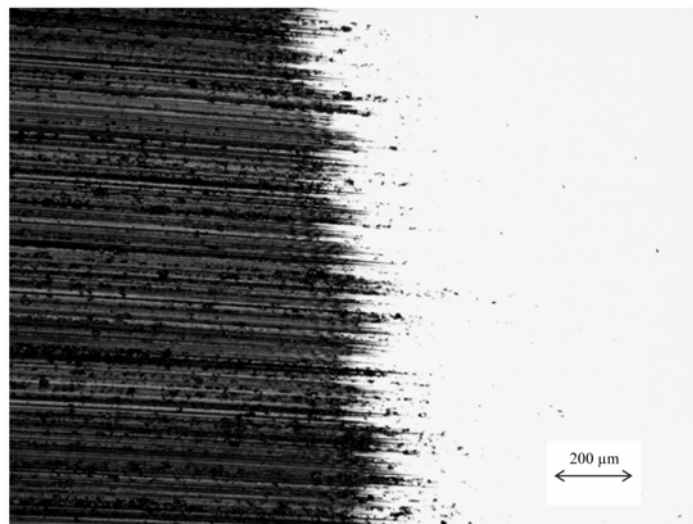


Table 3 Slanted polishing conditions

| Work material | Polishing time (hours) | |
|---|------------------------|------|
| | Ge | Si |
| Semifinishing/diamond paste 2–4 μm | 1.5 | 0.33 |
| Finishing/diamond paste 0.5 μm | 0.5 | 0.33 |

Figure 12 shows a micrograph of the surface polished using the slanted-polishing method. The grinding traces can be observed on the left side; while the right side is the crack-free area.

Figure 12 Micrograph of slanted polished germanium sample



5 Comparison between surface roughness and subsurface crack depth

The surface roughness and the crack depth of the ground surfaces of silicon evaluated by the above three methods were compared in Figure 13. The surface roughness data in the figure was measured using the $0.1 \times 2.5 \mu\text{m}$ stylus. It is clear that the crack depth values are bigger than the corresponding surface roughness values. Among all the three kinds of data, the crack depth measured by the slanted-polishing method is the biggest.

Figure 14 is a replot of crack depth data measured by small tool against surface roughness data in Figure 13. It can be seen that there is an approximate linear relationship between the crack depth and the surface roughness, which can be described by the following equation.

$$y = 2.2949x + 0.0177 \quad (3)$$

This equation shows that the crack depth is about 2.3 times the surface roughness results for silicon ground by various kinds of abrasives. Therefore, this relationship may be used to predict the subsurface crack depth from the surface roughness measurement results.

Figure 13 Plots of surface roughness and crack depths measured by two different methods versus diameter of abrasives used for grinding silicon

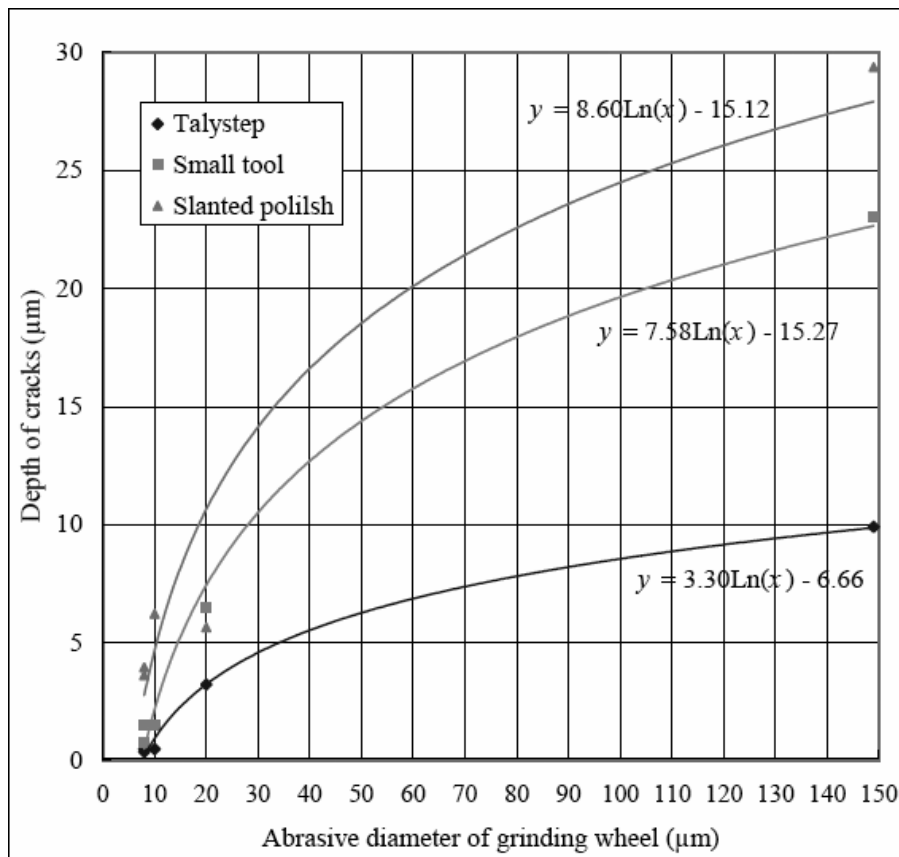
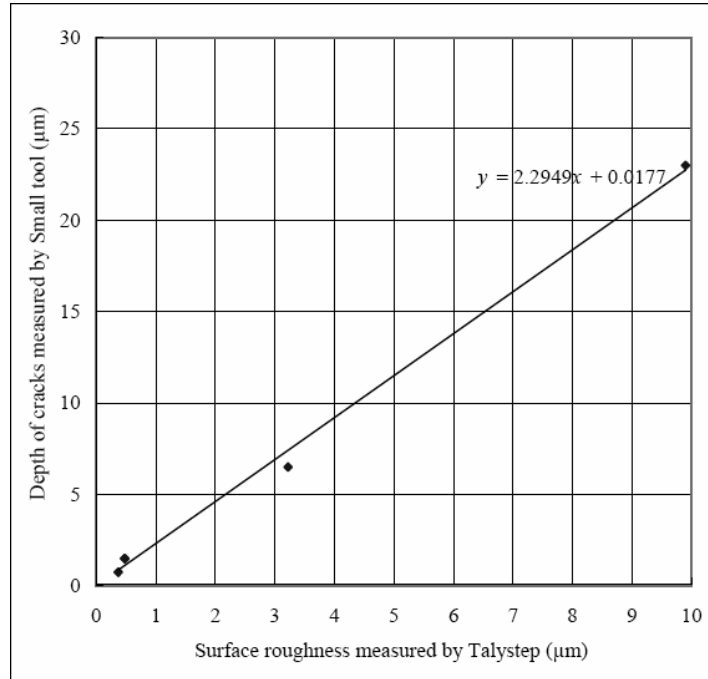


Figure 14 Plot of crack depth measured by small-tool polishing method versus surface roughness of ground silicon



On the other hand, it was also noted that the relationship between the crack depth measured by the slanted-polishing method and the surface roughness was non-linear but dependant on the size of grinding abrasives. As shown in Figure 13, the crack depth results of the 8- and 10- μm abrasives were about 10 times bigger than the surface roughness, whereas the crack depth results of the 20- and 149- μm diameter abrasives were about 3 times bigger than the corresponding surface roughness. This non-linearity might be due to that new microcracks have been generated or the grinding-induced cracks have been enlarged by the diamond abrasives during the slanted-polishing process. In this work, diamond paste of 0.5- to 4- μm abrasive was used for obtaining high material removal rates. If finer diamond paste is used, the linearity between the experimental data might be improved. In the small-tool polishing method, the diameter of the abrasive was much smaller, 0.08 μm and the hardness of the abrasive was also lower than diamond, thus the polishing process will not generate new cracks or enlarge existing microcracks.

Figure 15 shows the comparison results of germanium. In the figure, the crack depths measured by the slanted-polishing method and the surface roughness obtained by Talystep were plotted against the abrasive size. Figure 16 shows a replot of crack depth data against surface roughness data of Figure 15. It can be seen that, for germanium, the slanted-polishing method was successful. An approximate linear relationship exists between the two parameters, which can be described by Equation (4). From this equation, we can see that the crack depths were about 2.9 times the surface roughness for germanium.

$$y = 2.8779x + 0.5788 \quad (4)$$

Figure 15 Plots of surface roughness and crack depths measured by slanted-polishing method versus diameter of abrasives used for grinding germanium

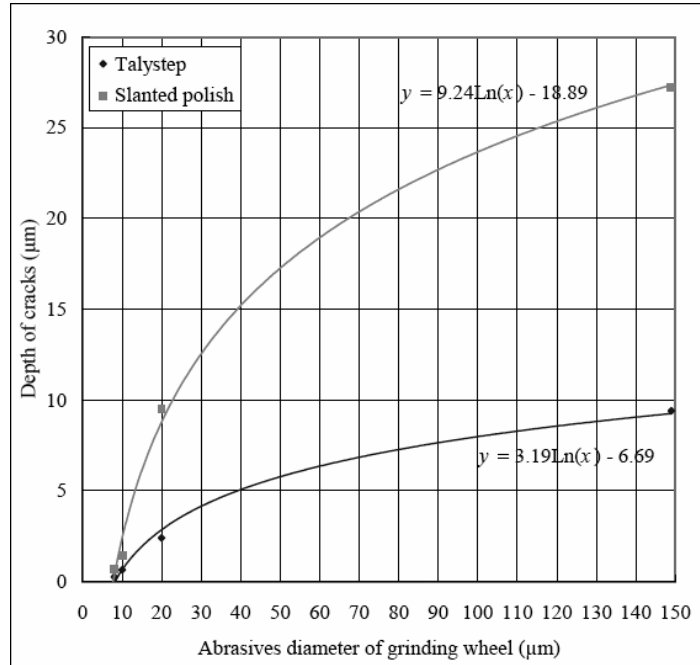
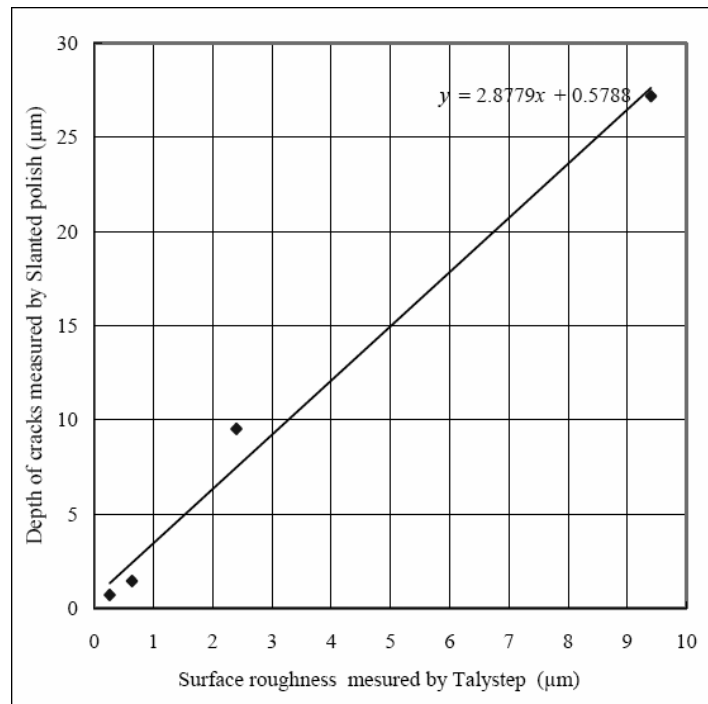


Figure 16 Plot of crack depth measured by slanted-polishing method versus surface roughness of ground germanium



A further comparison between Figures 14 and 16 indicates that the results of silicon and germanium are similar, not only in the trend of data relationship, but also in the values of crack depth. This fact implies that the subsurface damage depth and in turn, the subsurface fracturing mechanisms, of silicon and germanium are basically the same. For both materials, to remove the grinding-induced microcracks, the depth of cut for the finishing process should be at least 2–3 times bigger than the maximum surface roughness value R_y measured by the stylus profilometer.

6 Conclusions

The relationship between surface roughness and subsurface crack depth of ground silicon and germanium lens substrates was investigated. The subsurface crack depth was evaluated using two different methods, namely, small-tool polishing method and slanted-polishing method. The conclusions are shown below:

- 1 Maximum surface roughness and abrasive size have nearly a logarithmic relationship in the grinding of silicon and germanium.
- 2 The grinding-induced crack depth varies from 1 to 25 μm , depending on the size of abrasives. Abrasives finer than 10 μm are preferable for low-damage grinding.
- 3 Small-tool polishing with fine SiO_2 abrasives is an effective method to measure the subsurface crack depth of ground silicon; while for germanium, slanted polishing with diamond paste is also applicable.
- 4 Silicon and germanium have similar subsurface damage depth. For both of the two materials, the crack depth was 2–3 times bigger than the surface roughness measured by surface profilometer with a $0.1 \times 2.5 \mu\text{m}$ stylus.

The results from the present study have preliminarily demonstrated the feasibility of predicting the subsurface depth of the grinding-induced microcracks using the surface roughness results.

Acknowledgements

This work has been partially supported by the Industrial Technology Research Grant Programme (04A31508) from the Japan New Energy and Industrial Technology Development Organisation (NEDO).

References

- Matsui, S. (1999) 'Surface roughness of silicon wafers by wafer rotation grinding', *Journal of the Japan Society for Abrasive Technology*, Vol. 43, No. 10, p.43.
- Pei, Z.J., Billingsley, S.R. and Miura, S. (1999) 'Grinding induced subsurface cracks in silicon wafers', *International Journal of Machine Tools and Manufacture*, Vol. 39, No. 7, pp.1103–1116.
- Suzuki, H., Kodera, S., Nakasuji, T., Ohta, T. and Syoji, K. (1997) 'Study on aspherical surface polishing of single crystal silicon lens', *Journal of the Japan Society for Precision Engineering*, Vol. 63, No. 9, p.1280.

- Thomas, T.R. (1999) *Rough Surfaces*, Imperial College Press, p.20
- Yan, J. (2004) 'Laser micro-Raman spectroscopy of single-point diamond machined silicon substrates', *Journal of Applied Physics*, Vol. 95, No. 4, pp.2094–2101.
- Yan, J., Maekawa, K., Tamaki, J. and Kuriyagawa, T. (2005) 'Micro grooving on single-crystal germanium for infrared Fresnel lenses', *Journal of Micromechanics and Microengineering*, Vol. 15, pp.1925–1931.
- Yan, J., Syoji, K. and Kuriyagawa, T. (2002) 'Fabrication of large-diameter single-crystal silicon aspheric lens by straight-line enveloping diamond-turning method', *Journal of the Japan Society for Precision Engineering*, Vol. 68, No. 4, pp.1561–1565.
- Yan, J., Syoji, K., Kuriyagawa, T. and Suzuki, H. (2002) 'Ductile regime turning at large tool feed', *Journal of Materials Processing Technology*, Vol. 121, pp.363–372.
- Yan, J., Syoji, K. and Tamaki, J. (2003) 'Some observations on the wear of diamond tools in ultra-precision cutting of single-crystal silicon', *Wear*, Vol. 255, Nos. 7–12, pp.1380–1387.
- Yan, J., Takahashi, H., Tamaki, J., Gai, X. and Kuriyagawa, T. (2005) 'Transmission electron microscopic observation of nanoindentations made on ductile-machined silicon wafers', *Applied Physics Letters*, Vol. 87, No. 211901, pp.1–3.
- Yan, J., Yoshino, M., Kuriyagawa, T., Shirakashi, T., Syoji, K. and Komanduri, R. (2001) 'On the ductile machining of silicon for micro electro-mechanical systems (MEMS)', *Opto-Electronic and Optical Applications, Materials Science and Engineering A*, Vol. 297, Nos. 1–2, pp.230–234.
- Zhang, B., Zheng, X.L., Tokura, H. and Yoshikawa, M. (2003) 'Grinding induced damage in ceramics', *Journal of Materials Processing Technology*, Vol. 132, Nos. 1–3, pp.353–364.